https://dx.doi.org/10.4314/ijs.v26i2.4

EXPERIMENTAL AND COMPUTATIONAL STUDIES ON CORN-SILK DOPED MOLECULAR IMPRINTED POLYMER FOR THE SEQUESTRATION OF CRYSTAL VIOLET FROM AQUEOUS SOLUTION

Awokoya, K. N.[1,*], Oninla, V. O.[1], Akindoyin, G. O.[1], Famojuro, A. T.[1], Fakola, E. G.[1], Taleat, A. A. T.[2], and Ogunfowokan, A. O.[1]

[1]Department of Chemistry, Obafemi Awolowo University, Ile-Ife, 220007, Nigeria.
[2]Chemical Science and Technology Department, Federal Polytechnic, Ede, 232101, Nigeria.
[*]Corresponding Author's Email: knawokoya@oauife.edu.ng; knawokoya@gmail.com
(Received: 20th May, 2024; Accepted: 22nd July, 2024)

ABSTRACT

The capabilities of corn-silk doped molecularly imprinted polymer (CSDMIP) and its non-imprinted counterpart (CSDNIP), prepared using styrene as a functional monomer, in the adsorption of crystal violet (CV) dye were tested. The polymers were characterized by X-ray diffractometry (XRD), Fourier-transform infrared spectroscopy (FTIR), Thermogravimetry analysis (TGA) and scanning electron microscopy (SEM). The adsorbent potency in the dye removal was investigated by varying the effect of pH, time, dye concentration and temperature. A good removal efficiency of CV in the range of 95-99% was achieved for the imprinted polymer. Correlation coefficient R^2 value was the criterion in order to select the best kinetic and isothermal models. Pseudo-second-order model displayed a better fitness for kinetics data compared to the Elovich, Weber-Morris and pseudo-first order models. Likewise, Freundlich isothermal model depicted a better fit for the adsorption data for CV dye, demonstrating R^2 values of 0.9998 and 0.9999 for both CSDMIP and CSDNIP, respectively. The adsorption process was described as spontaneous and exothermic attributable to the negative thermodynamic parametrical values of ΔG^o and ΔH^o. In comparison to other selected adsorbents, CSDMIP was found more efficient with Langmuir adsorption capacity of 181.82 mgg^{-1}. In addition, the CSDMIP had an interestingly high reusability potential of >97% up to the sixth cycle. Computational study employed to validate the experimental analysis, gave a good result. Applicability of the developed adsorbent in real textile wastewater gave over 83% efficiency, suggestive of a promising adsorbent for the sequestration of CV from solution.

Keywords: Corn-silk; Density functional theory; Adsorption, Crystal violet, Imprinted polymer.

INTRODUCTION

Water is very essential for the sustenance of life on earth. However, only a little fraction of surface water (less than 3%) is suitable for human consumption. This is partly due to the vast influence of natural and man-made pollution on water accessibility (Padowski *et al.*, 2015; Wei *et al.*, 2021). Pollution of surface waters is caused by a number of matters, such as radioactive substances, putrescible organic waste and toxic chemicals etc. Among these toxic chemicals are dyes from various industries such as pharmaceutical, food processing, textile, carpet, plastics, cosmetics, paper, rubber, and leather (Tkaczyk *et al.*, 2020). The health implications of the release of these dyes and other toxic materials into water bodies are, therefore, matters of serious global concerns. For example, crystal violet (CV), a triphenylmethane and cationic dye with the chemical formula of $C_{25}H_{30}N_3Cl$, is classified as a mitotic poisoning agent and, consequently, is considered hazardous (Sarma *et al.*, 2016). Therefore, it is a matter of necessity to get it and other dyes of similar toxicity removed from industrial effluents.

In recent years, various conventional technologies and treatment procedures including biological treatments, chemical oxidation, photodegradation, reverse osmosis, coagulation-flocculation, Fenton/photo-Fenton, and adsorption have been employed by scholars for treating dye containing wastewater (Kapdan and Ozturk, 2005; Wahi *et al.*, 2005; Navarro *et al.*, 2019; Ghime *et al.* 2019; Elwakeel *et al.*, 2020a, 2020b; Awokoya *et al.*, 2021; Amigun *et al.*, 2022; Saleh *et al.*, 2021, 2022, 2023). Out of all these techniques, the adsorption process has been demonstrated to be sustainable, eco-friendly and effective. The process is simple and can be undertaken using a number of naturally available and renewable materials, thus making the process less or inexpensive (Yagub *et al.*, 2014; El-Kassimi *et al.*, 2018; Ahmed *et al.*, 2021). Many adsorbents

such as metal-organic frameworks, clay-organic composites, activated carbon, silica-based materials, biochar and agro-based materials like watermelon peel, banana peel, orange peel, plantain peel, garcinia kola pod and desert date seed shell have been investigated for their effectiveness in dye adsorption (Gao *et al.*, 2019; Santoso *et al.*, 2020; Ozola-Davidane *et al.*, 2021; Alam *et al.*, 2021; Oninla *et al.*, 2022). The effectiveness of most of these materials in sequestering dyes and other groups of pollutants from wastewaters have been reported. However, many of the materials have their drawbacks, which include low adsorption capacity, poor reusability and non-selectivity (Saxena *et al.*, 2020; Awokoya *et al.*, 2022).

Due to these drawbacks, molecular imprinting technology (MIT) has recently been considered a viable choice in adsorbent's preparation. This is owing to the excellent properties of the molecularly imprinted polymers (MIPs) synthesized by imprinting technology. These properties include high selectivity, robustness, long shelf life etc. (Zang *et al.*, 2012; Sharma *et al.*, 2012). MIPs are polymers that are prepared with predetermined selectivity, and they have found useful applications in many fields, such as chromatography, biosensing and solid phase extraction (Zhu *et al.*, 2019; Cantarella *et al.*, 2019). Nonetheless, MIPs are not without their own attendant drawbacks. These drawbacks are mainly associated with rigidity and limited number of high-affinity imprinting cavities (Ahamd *et al.*, 2015). Thus, simple and robust imprinting strategies that offer MIPs with less rigidity and a sizeable population of high-affinity imprinting cavities are required.

In this study, corn silk (CS), a residue from corn with little or no commercial value was used as a support matrix in the synthesis of MIP. CS is rich in a number of bioactive compounds including polyphenols (quercetin, hesperidin, vanillic acid and p-coumaric acid) and flavonoids (maysin) (Kaur *et al.*, 2022). The polyphenols and flavonoids present in the CS are considered to form non-covalent $\pi - \pi$ stacking interactions with styrene, divinyl benzene and CV template molecule, respectively. Although, in 2017, Petrović and his colleagues used pure CS to remove Cu^{2+} *and* Zn^{2+} from solutions containing these metal ions (Petrović *et al.,* 2017), to the best of the authors' knowledge, no work has yet been reported where CS is inserted to polymers using the MIT technique to synthesize MIP. Hence, for the first time, the use of CS doped MIP as an adsorbent for the sequestration of CV from an aqueous medium is here reported. Computational studies, employing the Density functional theory (DFT) method, was carried out to identify the template-monomer complexes that are most stable. Interaction energies (E_{t-m}) between the template molecule and the monomer styrene were also calculated. In addition, the reusability and stability of the synthesized MIPs were evaluated to explore the potential of practical applications for CV removal. Material characterization was accomplished by the use of spectroscopic techniques such as Fourier transform infrared spectroscopy (FTIR), scanning electron microscopy (SEM), X-ray diffractometry (XRD), and Thermogravimetry Analysis (TGA).

MATERIALS AND METHODS

Materials and corn silk preparation

The dye used, Crystal violet (CV) with molecular formula [$C_{25}H_{30}N_3Cl$], as well as other chemicals and reagents used, such as divinyl benzene (DVB), styrene (ST), benzoyl peroxide (BPO), acetic acid and methanol (MeOH) were procured from Sigma-Aldrich (Steinheim, Germany). All materials and chemicals were of analytical grade. Water was distilled at the Department of Chemistry, Obafemi Awolowo University (OAU), Ile-Ife, Nigeria. Fresh corn silk (CS) was sourced from a corn farm near the Postgraduate Hall, OAU, Ile-Ife, and identified (voucher specimen number: *IFE – 18213*) at the Botany Department, OAU, Ile-Ife, Nigeria. Impurities were removed from the surface of the CS sample by thorough washing with water. This was followed by oven drying at 80 °C. The dried CS sample was crushed with mortar and pestle, and then sieved using the sieve with mesh number of < 0.2 mm particle size.

Instrumentation

Characterization of the polymers was conducted by FTIR (Nicolet 330 spectrometer, Thermo Fisher Scientific, USA) within 4000 – 400 cm^{-1} to

investigate the functional groups. SEM images were taken to examine the morphology of its surface texture (SEM-EDX, Phenom ProX, Thermo Fisher Scientific, USA). TGA analysis was performed on *TGA – 4000*, PerkinElmer Analyzer, Waltham, MA, USA; while the XRD patterns of the polymers were obtained using Rigaku MiniFlex-600 and the diffractograms were recorded in the 2θ range $2^{o} – 70^{o}$.

Synthesis of corn-silk doped molecularly imprinted polymer (CSDMIP)

Corn-silk doped molecularly imprinted polymer (CSDMIP) was synthesized by bulk polymerization method, with the cationic dye (CV) as template molecule, according to the procedure reported by Awokoya *et al.* (2021), although with slight modification. The pre-polymerization components, which include 1.401 mmol template molecule (CV), 5.604 mmol styrene functional monomer (ST), 11.211 mmol crosslinker (DVB) and 0.5 mg initiator (BPO), were poured into a 100-mL standard flask containing 0.2 g of CS and 5 mL distilled water (porogen). The mixture (content of the 100-mL standard flask) was then stirred overnight for the complete dissolution of all solids. The resulting mixture was placed on a thermostatic hot plate set at 70^{o}C for 42 min for the complete polymerization reaction. After polymerization, a light purple solid polymer was obtained. This solid was crushed into powder using mortar and pestle. The optimized template-monomer mole ratio of 1:4 was used throughout this experiment. A similar experimental procedure was employed for the synthesis of corn-silk doped non-imprinted polymer (CSDNIP), used as a control adsorbent. The control adsorbent was prepared without the inclusion of the CV template molecule. Both adsorbents (CSDMIP and CSDNIP) were stored in different sealed plastic containers for further use.

Template extraction

The removal of CV template from CSDMIP was performed by continuous washing of the polymer with a mixture of acetic acid and methanol (1:9, v/v) until no trace of CV colour was noticed, and no CV signal was detected when analyzed using a UV–Vis spectrophotometer (Shimadzu UV-Vis-1800 model, Canby, Oregon, USA) at λ_{max} of 592 nm. Afterwards, the CSDMIP was filtered to obtain the "template-free" polymer. The residue (CSDMIP) was again thoroughly washed with absolute MeOH to eliminate acetic acid, and then air dried for 12 h. The principal goal of template removal was to generate cavities within the polymer matrix that can readily rebind the CV molecules from its solution and other complex media.

Application of CSDMIP/ CSDNIP in adsorption of CV

The CSDMIP/CSDNIP was applied as an adsorbent, and its efficacy in removing CV from an aqueous solution of the dye was investigated in a batch experiment process, using a thermostatic shaker with variable speed (GFL, Burgwedel, Germany). The study was performed in triplicate, and the average values were reported. A predetermined quantity (50 mg) of CSDMIP/CSDNIP was added to 20 mL of 50 mg/L^{-1} CV solution at pH values 1 to 9 in a series of 120 mL plastic vials. This was aimed at determining the optimum pH of the adsorption process, and the study was carried out at: 200 rpm (agitation speed), 1 h (agitation time), and 27 ℃ (process temperature). The influence of other parameters like contact time (5 to 240 min), initial CV dye concentration (5 to 200 mg/L) and temperature (30 to 60 ℃) on CV sequestration by the adsorbent materials were also evaluated. Separation of the spent adsorbent from solution was carried out by centrifugation at 6000 r/min for 5 min. Aliquots of the supernatant were drawn from the centrifuge tubes with the aid of a needle and syringe, and were analyzed for residual CV, using a UV–Vis spectrophotometer (Shimadzu UV-Vis-1800 model, Canby, Oregon, USA) at a peak wavelength of 592 nm. To confirm the desorption and reusability potentials of the CSDMIP, the solution containing CSDMIP (at CV concentration of 50 mg/L) was subjected to eight (8) adsorption-desorption cycles. Desorption experiment was carried out by treating the spent CSDMIP with a desorbing agent – a combination of MeOH and acetic acid (9:1, v/v). The extent of CV adsorption was expressed by evaluating the amount of the dye adsorbed per unit of adsorbent (Q_e) and the efficiency (E) of the dye removal as given in Eqs. (1) and (2),

respectively.

$$Q_e = \frac{(C_o - C_e)V}{m} \quad 1$$

$$E = \frac{C_o - C_e}{C_O} \times 100\% \quad 2$$

Where C_o *and* C_e denote initial and equilibrium CV concentrations (mgL^{-1}), V (in liters) represents volume of CV used, while m denotes mass of *CSDMIP or VSDNIP (g)*.

Modeling of the adsorption process

In an attempt to study the kinetics of CV adsorption onto CSDMIP/CSDNIP, four kinetic models – pseudo-first-order (PFO), pseudo-second-order (PSO), Elovich and Weber-Morris (W-M) (Lagergren 1898; Weber and Morris, 1963; Ho and Mckay 1999; Cheung *et al.* 2000) were employed; while for isothermal description, Langmuir, Freundlich and Dubinin-Radushkevich (D-R) models (Freundlich 1907; Langmuir 1918; Tempkin and Pyzhev, 1940; Dubinin *et al.* 1947) were considered to obtain information on the isothermal behaviour of the adsorption process. Evaluation of the spontaneity, endothermic/exothermic nature and the kind (physisorption or chemisorption) of adsorption involved was performed by interpreting the information obtained from the linear plot of the thermodynamic data. The van't Hoff equation, $\ln K_c = \frac{\Delta G^\circ}{R} - \frac{\Delta H^\circ}{RT}$, combined with thermodynamic relationships, such as $\Delta G^o = -RTlnK_c$ were used to derive the linear plot. Standard entropy changes (ΔS^o) and standard enthalpy change (ΔH^o) were then calculated. The Gibbs free energy change (ΔG^o) was valued according to the relationship: $\Delta G^o = \Delta H^o - T\Delta S^o$, where T stands for temperature (K). Gas constant, R, is represented by ($8.314\ Jmol^{-1}K^{1}$), while the equilibrium constant, K_c, is defined as $\frac{C_a}{C_e}$ where C_a indicates CV concentration on the adsorbent (CSDMIP/CSDNIP) at equilibrium.

Computational studies

A computational study was employed in this study to select the optimal template-monomer mole ratio best suitable for the polymer synthesis. Quantum calculations in this study were conducted using Spartan 14 software. The DFT method at the B3LYP level, employing the 6-31G* basis set, was employed for geometry optimization and determination of the HOMO (highest occupied molecular orbital) and the LUMO (lowest unoccupied molecular orbital) energy levels (Awokoya *et al.*, 2022). The optimized conformations for the styrene (monomer) and crystal violet (template) are presented in Figure 1.

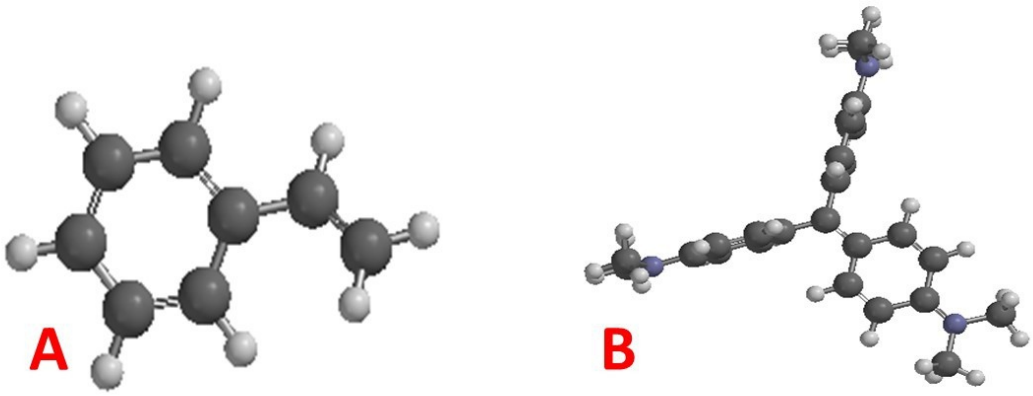

Figure 1: Optimized conformations of styrene (A) and CV (B) molecule

The binding energies between crystal violet and styrene were quantified by single-point calculations, utilizing equation (3).

$$\Delta E_{ads} = E_{t\text{-}m} - E_t - \Sigma E_m \quad 3$$

where E_{t-m} represents total energy of energy CV (template) and styrene (monomer) molecules, *Et* represents the energy of the template molecule, while *Em* denotes the cumulative energy of the monomer. The quantum parameters (electronic) computed in this study includes energy gap (ΔE), chemical potential (μ), chemical hardness (η), and fractional number of transferred electrons between adsorbate and adsorbent (ΔN). The quantum parameters, which were later used to predict the adsorption mechanisms, were computed using equations 4, 5, 6, and 7 (Okoli *et al.*, 2014).

$$\eta = \frac{1}{2}(E_{LUMO} - E_{HOMO}) \quad 4$$

$$\mu = \frac{1}{2}(E_{HOMO} + E_{LUMO}) \quad 5$$

$$\Delta E = E_{LUMO} - E_{HOMO} \quad 6$$

$$\Delta N = \frac{\mu_B - \mu_A}{2(\eta_B - \eta_A)} \quad 7$$

The frontier molecular orbitals energy is represented as E_{LUMO} and E_{HOMO}. Symbols, μ_A and μ_B depict the chemical potentials of the adsorbent and adsorbate, respectively, while η_A and η_B symbolizes the chemical hardness of the adsorbent and adsorbate, respectively.

RESULTS AND DISCUSSION

Characterization of CSDNIP and CSDMIP

The FTIR spectra of ***CSDNIP, CSDMIP$_{Before}$ and CSDMIP$_{After}$*** (corn silk doped molecularly imprinted polymer before and after adsorption) were recorded in the wavenumber range of ***400 – 4000 cm^{-1}*** as depicted in Figure 2A. The three spectra showed several similar peaks that revealed different functional groups. Thus, the similarity in peaks for all the polymers is ascribed to the same pre-polymerization contents present in the polymer matrix. The broad vibrational peak between ***3437 – 3460 cm^{-1}*** in all the polymers is attributed to the OH stretching vibration of water which was used as porogen in the synthesis of the polymers. The peaks at ***2924 cm^{-1}, 1315 – 1384 cm^{-1}, 1454 – 1543 cm^{-1}, and 1716 -1747 cm^{-1}*** have been attributed to ***C H*** stretching, aromatic ***CH$_3$,*** aromatic ***C = C*** and ***C = O*** vibrations, respectively (Awokoya *et al.*, 2024). However, it is pertinent to note that upon CV adsorption, the peak at ***1724 cm^{-1}*** for both ***CSDNIP$_{Before}$ and CSDMIP$_{After}$*** shifted towards a higher wavenumber of ***1747 cm^{-1}***. This shift is evidence of the interaction between the polymer and the CV molecules in the adsorption process. In addition, the sawtooth characteristic peaks at ***1030 – 1180 cm^{-1}*** has been assigned to ***C O*** stretching vibrations which confirms the presence of the benzoyl peroxide initiating molecule in all the polymers.

The SEM micrographs obtained for ***CSDNIP, CSDMIP$_{Before}$ and CSDMIP$_{After}$*** are shown in Figure 2B. Clearly, fibrous and homogeneous size textures were observed in all the micrographs with ***CSDNIP*** having a rougher surface compared to ***CSDMIP$_{Before}$ and CSDMIP$_{After}$***. The ***CSDMIP$_{Before}$*** remains almost unchanged upon the adsorption of CV, which may be an indication that the CV adsorbate was homogeneously dispersed in the ***CSDMIP$_{After}$*** matrix. XRD analysis was performed to ascertain the degree of the amorphousity/crystallinity of ***CSDNIP, CSDMIP$_{Before}$ and CSDMIP$_{After}$***. As illustrated in Figure 3A. One major broad and notable diffraction peak at 2 = 20.24° in all the samples, represents the crystalline domain of the polymers. Also, a particular hump was observed at 2 = 12.34° in all the polymers. The similarity in the XRD patterns of the polymers indicates that the adsorption of CV on the adsorbents has no significant effect on the crystallinity or amorphousity of the polymer materials. Overall, one can infer that the corn-silk doped polymers produced in this study are highly porous and amorphous. Thus, the amorphous characteristic can be attributed to the corn-silk biomaterial (natural polymer) embedded into the synthetic polymer (Lata, 2017).

TGA analysis was conducted to evaluate the thermal stability and the rate of the decomposition of the synthesized polymers at elevated temperatures. As revealed in the thermogram (Figure 3B), two different stages of

mass loss were observed for $CSDMIP_{Before}$ *and* $CSDMIP_{After}$, while four regimes of mass loss were detected for *CSDNIP*. The first weight loss was observed at a temperature below 200 °C for the three polymers, with a loss of about 3.7%. This first mass loss stage has been ascribed to the loss of moisture and some other volatile compounds, as well as attrition of functional groups, such as *OH* and *CO* on the imprinted polymer backbone (Idris-Hermann *et al.*, 2018; Roland *et al.*, 2019; Kulal and Badalamoole, 2020; Awokoya *et al.*, 2021). The second stage, which is the main decomposition stage began around 300 °C for both $CSDMIP_{Before}$ *and* $CSDMIP_{After}$, and 330 °C for *CSDNIP*, with gradual degradation until 400 °C for $CSDMIP_{Before}$ and 520 °C for $CSDMIP_{After}$. The third stage of decomposition started at a temperature of 390 °C for *CSDNIP*, after which stability was observed from 440 - 690 °C. The fourth and slight weight loss (about 1%) observed at 700 °C most likely originated from the non-existence of cavities on the *CSDNIP* adsorbent. For the three samples, a good thermal stability as high as 300 °C was discovered, thus, suggesting the conferment of strength and stability on the synthesized materials by DVB crosslinker. This most possibly allowed the materials to possess the ability to withstand more heat.

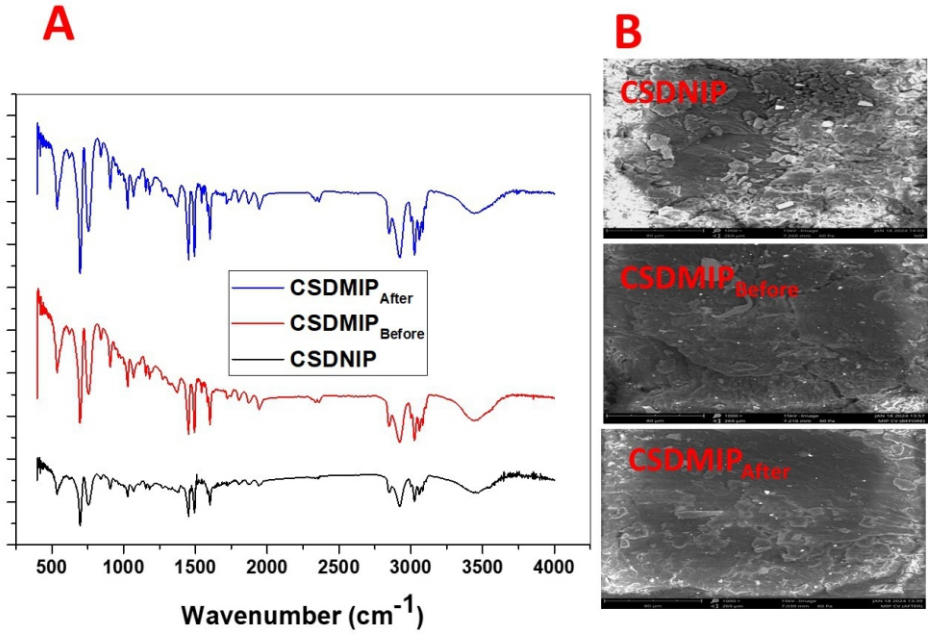

Figure 2: *FTIR* spectra (**A**) and SEM images (**B**) of the polymers

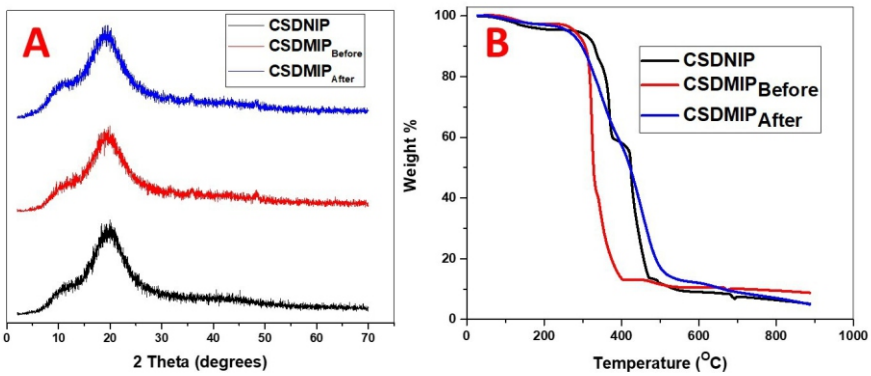

Figure 3: *Curves of (**A**) XRD and (**B**) TGA of CSDNIP,* $CSDMIP_{Before}$ *and* $CSDMIP_{After}$ *polymers*

Adsorption studies

Investigation of the effect of pH on CV dye removal

The pH of an aqueous solution is a key operational parameter that strongly affects the surface charge of an adsorbent, and the magnitude of adsorbate ionization. The efficiencies of the removal of CV dye by CSDMIP and CSDNIP over a pH range of 1 to 9 (with other operational parameters fixed – time: 60 min, adsorbent dose: 0.05 g, concentration: 50 mg/L and temperature: 27 ^{o}C $\pm$ 1) are graphically represented as shown in Figure 4a. Although the dye removal by the two polymer materials was observed to follow a similar trend, nevertheless, CSDMIP was discovered to be almost 2 times more efficient than CSDNIP at all the pHs considered. The CV removal efficiencies increased with an increase in pH from 1 to 6, with the maximum efficiencies (> 96%) for CSDMIP and (> 48%) for CSDNIP at pH 6. This increment trend can be ascribed to the increase in the magnitude of the electrostatic attractive force between the dye and the adsorbent surface as pH was raised (Monash and Pugazhenthi, 2009). However, with an increment of pH from 6 to 9, the amount of CV adsorbed reduced slightly with the removal efficiency dropping from 96.8 to 94.9% for CSDMIP and 48.4 to 45.5% for CSDNIP. The gradual reduction in CV removal at pH above 6 could be ascribed to the decreased negative charge density on the adsorbent surface, resulting in repulsion between the CSDMIP/CSDNIP and the positively charged CV molecule. Hence, for subsequent studies, pH 6 was adopted for all experiments.

Investigation of the effect of contact time and the adsorption kinetics

Varying the interaction time between the adsorbent and the pollutant molecules in aqueous solution has been reported to have a crucial effect on adsorption. The study to investigate the effect of the period of interaction between the adsorbents and CV was conducted at ten different times – from 5 to 240 min, while CV concentration, adsorbent dosage, pH and temperature were kept constant. As illustrated in Figure 4b, it was observed that the removal efficiency increased rapidly in the first 30 min and then slightly slowed down after 30 min until stability (equilibrium) was attained at 60 min. After 60 min of contact, about 47.9 and 95.1% CV removal efficiencies was obtained for CSDNIP and CSDMIP, respectively. This possibly suggests that the cavities (binding sites) on the polymers were nearly saturated at 30 min, and then reached an adsorption equilibrium phase, where all the cavities became occupied, after 60 min. The observed quick adsorption could possibly be as a result of high CSDMIP – CV interactions affinity. Further increase in contact time until 240 min did not give any meaningful change in the removal efficiency. Hence, 60 min was selected as the best equilibrium time for further studies.

Kinetic parameters obtained from the modelling of the process with pseudo-first-order, pseudo-second-order, weber-morris, and elovich models are recorded in Table 1. The suitability of the model was established using the correlation coefficient (R^2). With R^2 values of unity for both CSDMIP and CSDNIP, it can be predicted that the PSO kinetic model was more suitable and applicable to fit data from the adsorption of CV onto both polymers. In addition, the extremely close agreement between the experimental and calculated ($q_{e(exp)}$ = 14.6413 and $q_{e(calc)}$ = 14.6422 for CSDMIP; while $q_{e(exp)}$ = 10.9170 and $q_{e(calc)}$ = 10.9391 for CSDNIP) further strongly validates that the PSO model best defines the process of the adsorption of CV. The R^2 values for PFO and W-M were far lower (0.5634 to 0.6512 and 0.7044 to 0.7744 respectively) compared to the PSO model. It is important to note that the $q_{e(calc)}$ values (12.008 to 21.488) for PFO were far different from the $q_{e(exp)}$ = (0.043 to 0.062) values. In the case of Elovich, the resultant R^2 values of about 0.9277 to 0.9281 approach unity, thus offering a better fitting compared to PFO and W-M models. The R^2 demonstrated the following order to the fitted kinetic models: ***PSO > Elovich > WM > PFO***. This result predicts chemisorption as the rate determining step in the adsorption of CV onto CSDMIP/CSDNIP polymers. In addition, the Elovich model principally depicts chemisorption and predominantly effective in the description of a heterogeneous adsorbing surface; thereby strongly affirming the involvement of chemisorption (Cheung *et al.*, 2000; Tan, *et al.*,

2017). Awokoya *et al.* (2024) reported a similar finding for the adsorption of bromocresol green dye using trimethoprim vanillin anchored conjugate imprinted polymers.

Investigation of the effect of initial CV concentration and adsorption isotherms

The profound effect of initial concentration on CV removal by CSDMIP/CSDNIP was studied (Figure 4c). Adhesion of CV on CSDMIP increased from 96.8 to 98.6%, and 46.9 to 49.0% for CSDNIP with a rise in initial CV concentration from 5 – 50 mgL^{-1}. At the initial concentration of 100 mgL^{-1}, about 99.0% of the CV was observed to have been removed by CSDMIP. On the other hand, at the highest CV initial concentration considered in this study (200 mgL^{-1}), only about 50.2% removal efficiency was recorded when CSDNIP was applied. The increase in uptake with a rise in initial CV concentration could be attributed to a possible increasing driving force that overpowered the mass transfer resistance of CV from the bulk solution to the CSDMIP/CSDNIP surface. The isothermal behavior of the adsorption of CV onto CSDMIP/CSDNIP was examined using four different models. Equilibrium parameters from these models are presented in Table 2. The model that best fits the process was chosen based on the closeness of its R^2 to unity. The adsorption of CV by both CSDMIP and CSDNIP best fitted the Freundlich model: R^2 = 0.9998 and 0.9999 for CSDMIP and CSDNIP, respectively. This suggests the involvement of a heterogenous adsorbent surface during the sequestration of CV. It should also be pointed out that the R^2 values close to unity were obtained for both Langmuir (0.9992 and 0.9938) and Dubinin-Radushkevich (0.9724 and 0.9806) models. For both polymers, the order of fitting for the isotherm models followed the trend: Freundlich > Langmuir > Dubinin > Radushkevich > Temkin. Furthermore, in the D-R model, the E (mean free energy) values for both polymers were 14.08 and 14.39 kj mol^{-1} (>8 kj mol^{-1}), indicating that the adsorption of CV by CSDMIP/CSDNIP followed chemisorption, with possible involvement of chemical ion exchange mechanism. This observation lends credence to adsorption kinetic results. Also, the Langmuir maximum adsorption capacity of CV dye molecule on the CSDMIP was 181.82 mg g^{-1}. When compared with other selected adsorbent materials (Table 4), it becomes apparently clear that CSDMIP has a promising adsorptive property. In view of this, one could infer that, CSDMIP is a valuable adsorbent for cationic dyes like CV.

Investigation of the effect of temperature and the thermodynamics of the process

The adsorption of CV onto CSDMIP/CSDNIP was conducted at different temperatures as depicted in Figure 4d. The calculated thermodynamic parameter values are also presented in Table 3. Based on the obtained results, as the temperatures rises from 303 – 333K, the adsorption performance decreases and the highest removal efficiencies were 98.7% for CSDMIP and 49.6% for CSDNIP at 303K. The decrease in the removal efficiency with increase in temperature is an indication of an exothermic process (Awokoya *et al.* 2024). This was corroborated by the negative value of ΔH°. In addition, the ΔG° values for both polymers at the studied temperatures were negative, demonstrating the spontaneity and feasibility of CV adsorption onto CSDMIP/CSDNIP. The positive value of ΔS° for CSDNIP shows the affinity of CSDNIP for CV, and it suggests a fast adsorption process (Kolodynska *et al.* 2017). Conversely, the negative value of ΔS° for CSDMIP indicates a decrease in disorderliness (Chakraborty *et al.* 2005).

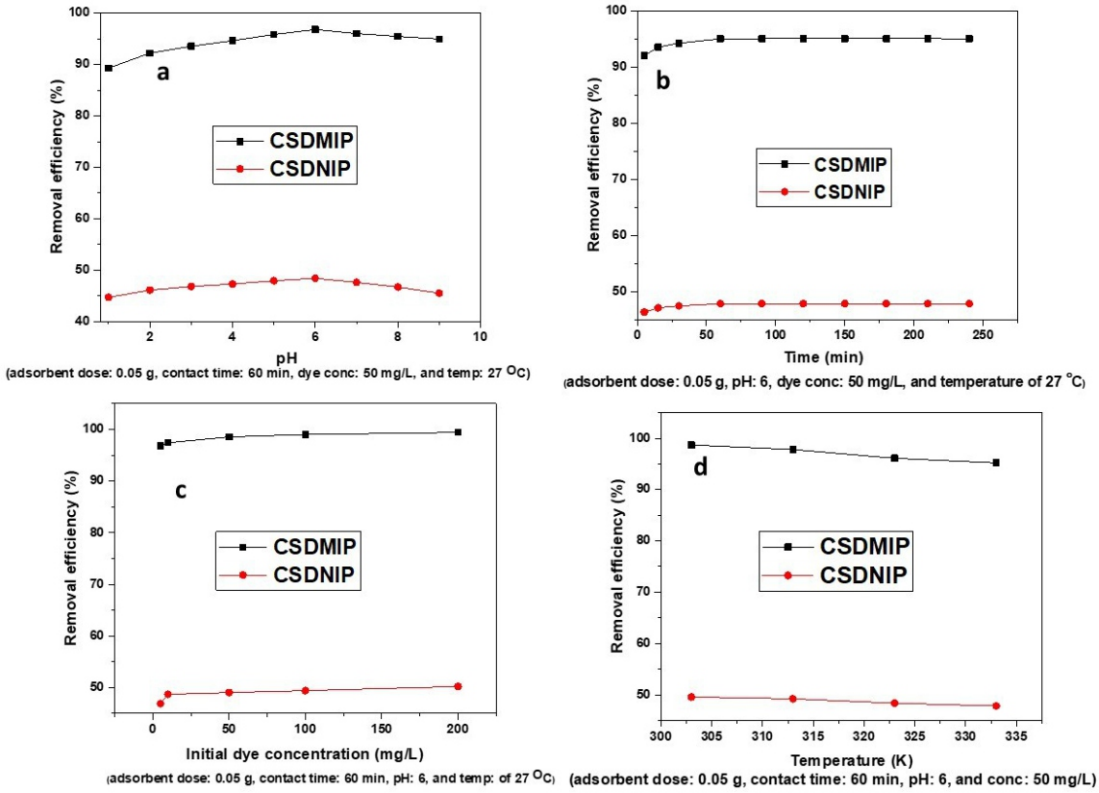

Figure 4: Effects of different operational parameters: (a) pH, (b) contact time (c) initial dye concentration and, (d) temperature on CV removal by CSDMIP/CSDNIP

Table 1: Linearized kinetic equations and the calculated values of their parameters

Model	Equation	Parameter	CSDMIP	CSDNIP	Definition
PFO	$\ln(q_e - q_t) = \ln q_e - k_1 t$	R^2	0.6512	0.5634	q_t: amount of dye adsorbed
		k_1 (L/min)	0.0190	0.0102	k_1: PFO rate constant
		$q_{e(exp)}$ (mg/g)	0.062237	0.043149	t: time
		$q_{e(calc)}$ (mg/g)	21.488	12.008	
PSO	$\frac{t}{q_t} = \frac{t}{q_e} - \frac{1}{k_2 q_e^2}$	R^2	1.0000	1.0000	
		k_2 (g/mg. min)	0.6304	1.2713	K_2: PSO rate constant
		$q_{e(exp)}$ (mg/g)	14.6413	10.9170	
		$q_{e(calc)}$ (mg/g)	14.6422	10.9391	
W-M	$q_t = k_\alpha t^{1/2} + C$	R^2	0.7740	0.7044	k_α: W-M rate constant
		k_α (mg/g. $min^{1/2}$)	0.0213	0.0107	C: intercept
		C	14.399	10.804	
Elovich	$q_t = \frac{1}{\beta}\ln[\alpha\beta] + \frac{1}{\beta}\ln t$	R^2	0.9281	0.9277	α: initial adsorption rate
		α (mg/g. min)	1.1 E+87	1.6E+131	β: desorption constant
		β	14.206	28.409	

Table 2: Isothermal model and their parameters for the sequestration of CV by CSDMIP and CSDNIP

Isotherm	Equation	Parameter	CSDMIP	CSDNIP	Definition
Langmuir	$\frac{1}{q_e} = \frac{1}{q_{max}K_{LC_e}} + \frac{1}{q_{max}}$	R^2	0.9992	0.9938	K_L: Langmuir constant
		k_L (L/mg)	0.004	1.043	q_{max}: maximum dye adsorbed
		q_{max} (mg/g)	181.82	16.502	
Freundlich	$\ln q_e = \ln k_F + \frac{1}{n}\ln C_e$	R^2	0.9998	0.9999	n: heterogeneity factor
		k_F (L/mg)	88.464	0.701	k_F: Freundlich constants
		1/n	1.7876	1.0241	
D-R	$\ln q_e = \ln q_m - \beta\varepsilon^2$	R^2	0.9724	0.9806	q_m: maximum dye adsorbed
	$\varepsilon = RT\ln\left(1+\frac{1}{C_e}\right)$	q_m (mmol/g)	6 E+3	69.33	β (mol^2/kJ^2): D-R constant
	$E = \frac{1}{\sqrt{2\beta}}$	E (kJ/mol)	14.08	14.39	ε (J/mol): Polanyi potential
					R (8.314 J/mol. K): gas constant
					T (K): Temperature
					E: Energy
Temkin	qe = B ln K_T + B ln Ce	R^2	0.6972	0.8164	K_T: Temkin adsorption potential
		K_T(L/g)	6.3858	0.3295	B= RT/b: Temkin constant
		b (kJ/mol)	20.56	54.94	

Table 3: Thermodynamic quantities estimated for CV adsorption onto CSDMIP and CSDNIP

Adsorbent	ΔH (kJ/mol)	ΔS (kJ/mol.K)	ΔG(kJ/mol)			
			303 *K*	313 *K*	323 *K*	333 *K*
CSDMIP	−38.924	−0.087	−12.55	−11.68	−10.81	−9.94
CSDNIP	−1.435	0.002	−2.04	−2.06	−2.08	−2.10

Table 4: Comparison of Langmuir adsorption capacity of CSDMIP with selected adsorbent materials

Adsorbent materials	Dose (g)	$Conc\ (mg\ L^{-1})$	$q_{max}\ (mg\ g^{-1})$	
			CV	
This study	0.05	$5-200$	181.82	
Peanut husk	*0.5*	$100-450$	20.0	(Abbas *et al.* 2021)
Calligonum comosum leaf powder	*0.5*	$100-500$	-0.571	(Alsenani 2021)
Xanthated rice husks	0.025	50	90.02	(Homagai *et al.* 2022)
Activated carbon/Fe_3O_4	*0.5*	$10-80$	35.31	(Foroutan *et al.* 2021)

Regeneration studies

In addition to sensitivity and selectivity, two salient characteristics of any good adsorbent are reusability and stability. As depicted in Figure 5, the results of the reusability of CSDMIP shows that the polymer is readily reusable for up to six cycles with the removal efficiency of about 97.26% without a significant drop in its adsorption potency. After the sixth cycle time, the removal efficiencies slightly decreased to 95.33% and 92.11% at the seventh and eighth cycles, respectively. It could be seen that CSDMIP adsorbent can be used repeatedly after regeneration, thus, lowering waste creation and making imprinted polymer adsorbents advantageous for industrial applications.

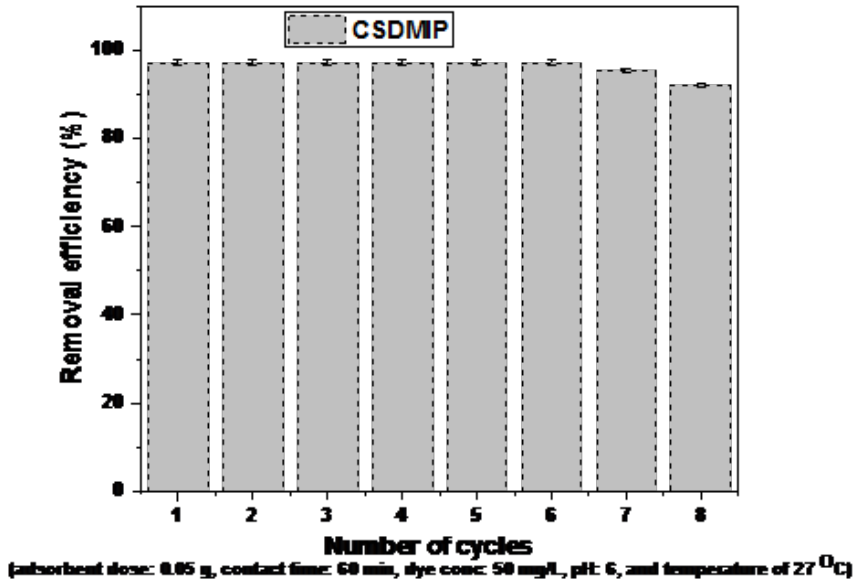

Figure 5. Removal efficiencies of CSDMIP in eight consecutive regeneration cycles.

Validation

The potency of the developed adsorbent (CSDMIP) was validated by applying the material on the real textile wastewater sample collected from Ibadan City, Nigeria. Removal efficiency above 83% was attained for the CV dye molecule. This appealing feature makes CSDMIP a potential adsorbent for practical application in real-time wastewater treatment.

Quantum chemical studies

The investigation focused on template-monomer interactions to identify the template-monomer complexes that are mostly stable, and compute their electronic stabilization energy. The optimized geometries of template-monomer complexes, considering molar ratios of 1:1, 1:2, 1:3, 1:4, and 1:5, were determined under vacuum conditions. The structures of the complexes and the DFT electronic parameters are shown in

Figure 6 and Table 5, respectively.

The results revealed that the highest stability of the template-monomer complexes was obtained at mole ratio 1:4 (ΔE = 1.72 eV), thus, suggesting that 1:4 molar ratio of crystal violet-styrene mixture would be the most suitable ratio for the synthesis of CSDMIP. Reduced ΔE values signify diminished stability and heightened reactivity of the complex, while an increased ΔE value indicates enhanced stability and reduced reactivity (Okoli *et al*. 2014; Platts & Baker, 2020). In addition, Binding energies (ΔE_{ads}) for the complexes crystal violet styrene ($CVST_1$ to $CVST_5$) show increasing interaction strength as more monomers bind to the template. The binding energy for $CVST_1$ is -0.06 eV, indicating a weak interaction with one monomer. This increases to -0.24 eV for $CVST_2$, suggesting a stronger interaction with two monomers. For $CVST_3$, $CVST_4$, and $CVST_5$ the binding energies are -0.22, -0.34, and -0.31 eV respectively. The strongest binding energy is observed in $CVST_4$ at -0.31 eV. The η, μ and ΔN quantum descriptors are equally significant in predicting and understanding adsorption interactions between adsorbents and adsorbates (Awokoya *et al*.,2022; Bisiriyu and Meijboom, 2020; Khnifira *et al*., 2022; Huang and Zhu, 2015). The value of ΔN > 0 (0.93) obtained for the complexes strongly suggests that the adsorbent was likely to have donated electrons (Obot *et al*. 2015). Thus, there is a higher possibility of charge transfer (flow) from the adsorbent to the adsorbate. Apparently, this may be the main mechanism of the process. The exact link between adsorption and chemical potential (μ) has not been well- established in the literature with nearly most adsorption processes reported to favour lower μ as observed in this study (Table 1). In addition, the value of η in all the complexes in the range of 0.71 – 0.86 shows that there is interaction and stability between the adsorbent and the adsorbate because chemical stability and reactivity are associated with chemical hardness (Kasera, *et al*. 2023).

Table 5: Estimated DFT quantum electronic parameters

Compounds	**E (eV)**	**E_{HOMO} (eV)**	**E_{LUMO} (eV)**	**ΔE(eV)**	**η (eV)**	**μ(eV)**	**ΔN**
Styrene (ST)	-8425.92	-6.13	-0.63	5.5	2.75	-3.38	
Crystal violet (CV)	-30877.6	-7.32	-5.84	1.48	0.74	-6.58	
$CVST_1$	-39303.6	-7.21	-5.79	1.42	0.71	-6.50	
$CVST_2$	-47729.7	-7.22	-5.66	1.56	0.78	-6.44	0.93
$CVST_3$	-56155.6	-7.24	-5.66	1.58	0.79	-6.45	
$CVST_4$	-64581.6	-7.23	-5.51	1.72	0.86	-6.37	
$CVST_5$	-73007.5	-7.03	-5.50	1.53	0.77	-6.27	

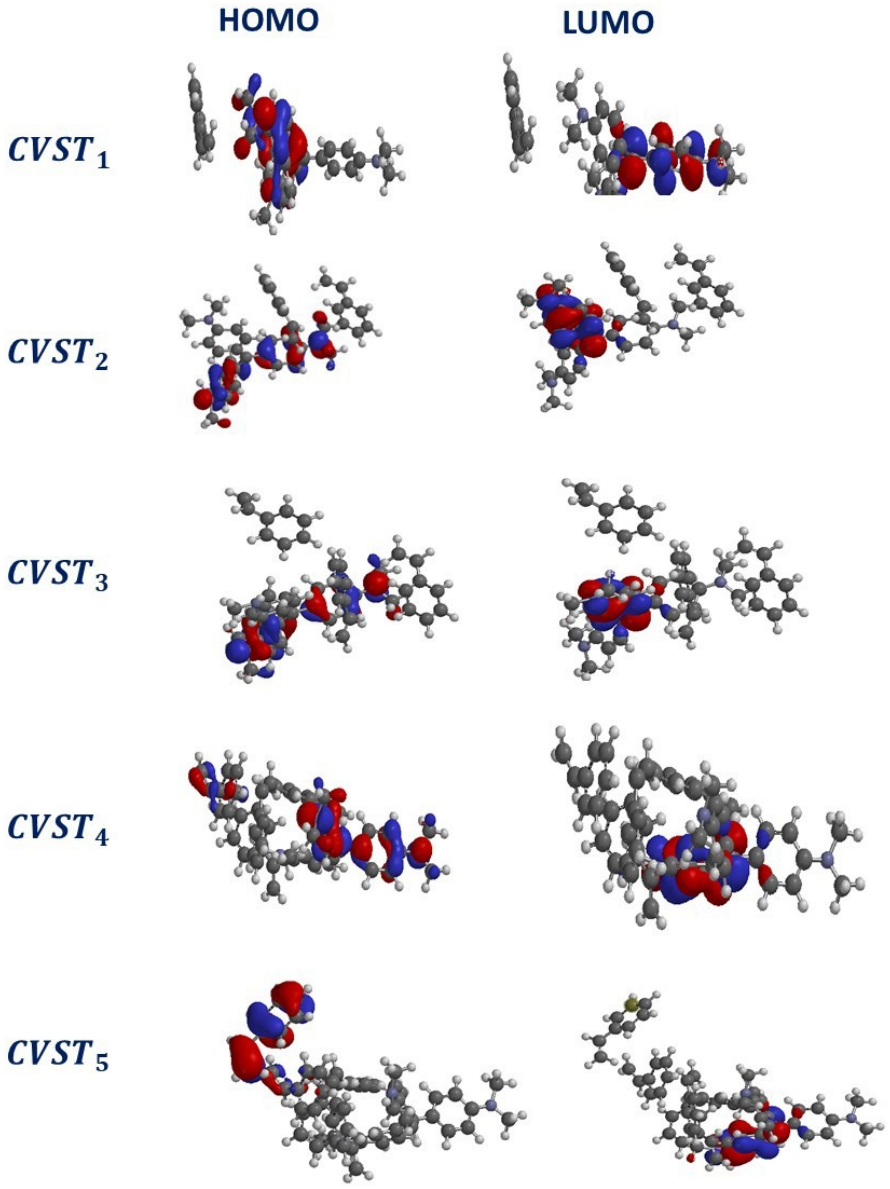

Figure 6: HOMO and LUMO molecular orbitals calculated for the tested $CVST_1$ $CVST_5$ complexes.

CONCLUSION

A highly selective and effective corn-silk doped molecularly imprinted polymer was synthesized, with the objective of removing CV from an aqueous solution. Sixty (60) min of contact with the solution and 50 mg of CSDMIP were sufficient to attain high removal efficiency of above 95%. The experimental data were best defined by pseudo-second-order kinetic model. Concentration data was found to follow closely the Freundlich model with R^2 values in the range of 0.9998 0.9999. Investigations of temperature profiles suggest an exothermic process, and the negative value obtained for ΔG° showed that the CV removal process was spontaneous. The results of the SEM, FTIR, TGA and XRD analyses all predicted the affinity of the studied CSDMIP for the CV dye. Hence, these findings assert that the synthesis of corn-silk doped imprinted material is economically feasible, and could be efficiently used as a selective adsorbent for the removal of CV from aqueous solutions.

ACKNOWLEDGEMENTS

The authors appreciate the Polymer Science and Biophysical Chemistry Laboratory for given access to their laboratory

FUNDING AND/OR CONFLICTS OF INTERESTS/COMPETING INTERESTS

We would like to state unequivocally that there are no known conflicts of interest associated with this manuscript. No funding from any source was received. No competing interest of any kind.

REFERENCES

Abbas S, Javeed T, Zafar S, Taj MB, Ashraf AR, Din MI (2021) Adsorption of crystal violet dye by using a low-cost adsorbent – peanut husk. *Desalination and Water Treatment* 233: 387–398. doi: 10.5004/dwt.2021.27538

Ahmad AL, Lah NFC, Chun S (2015) Low molecular imprinted polymer for atrazine detection sensor: Preliminary study. *Chemical Engineering Transactions* 45: 1483e1488. doi: 10.3303/CET1545248

Alam S, Barkat U, Muhammad SK, Najeeb R, Luqman K, Luqman AS, Ivar Z, Juris B, Anna K, Nikolai P *et al*. (2021) Adsorption, Kinetics and Isotherm Study of Basic Red 5 on Synthesized Silica Monolith Particles. *Water* 13: 2803. doi: 10.3390/w13202803

Alsenani G (2021) Studies on adsorption of crystal violet dye from aqueous solution onto calligonum comosum leaf powder. *Journal of American Science* 17: 70-75. doi:10.7537/marsjas170321.09

Amigun AT, Adekola FA, Tijani JO, Mustapha S (2022) Photocatalytic degradation of malachite green dye using nitrogen/sodium/iron-TiO_2 nanocatalysts. Results Chem 4: 100480. doi: 10.1016/j.rechem.2022.100480

Awokoya KN, Oninla VO, Bello DJ (2021) Synthesis of oxidized Dioscorea dumentorum starch nanoparticles for the adsorption of lead (II) and cadmium (II) ions from wastewater. *Environmental Nanotechnology, Monitoring & Management* 15: 100440. doi: 10.1016/j.enmm.2021.100440

Awokoya KN, Okoya AA, Elujulo O (2021) Preparation, characterization and evaluation of a styrene-based molecularly imprinted polymer for capturing pyridine and pyrrole from crude oil. *Scientific African* 13: e00947. doi: 10.1016/j.sciaf.2021.e00947

Awokoya KN, Oninla VO, Adeyinka GC, Ajadi MO, Chidimma OT, Fakola EG, Akinyele OF (2022) Experimental and computational studies of microwave-assisted watermelon rind–styrene based molecular imprinted polymer for the removal of malachite green from aqueous solution. *Scientific African* 16: e01194. doi: 10.1016/j.sciaf.2022.e01194

Awokoya KN, Oninla VO, Eugene-Osoikhia TT, Njionye UO, Okoya AA, Adeyinka GC, Odor C (2024) Synthesis of trimethoprim vanillin anchored conjugate imprinted polymers for removal of bromocresol green and malachite green from aqueous media. *Water Science and Engineering*. doi: 10.1016/j.wse.2024.01.004.

Bisiriyu IO, Meijboom R (2020) Adsorption of Cu (II) ions from aqueous solution using pyridine-2, 6-dicarboxylic acid crosslinked chitosan as a green biopolymer adsorbent. International *Journal of Biological Macromolecules* 165: 2484-2493. doi: 10.1016/j.ijbiomac.2020.10.150

Cantarella M, Carroccio SC, Dattilo S, Avolio R, Castaldo R, Puglisi C, Privitera V (2019) Molecularly imprinted polymer for selective adsorption of diclofenac from contaminated water. Chem Eng J 367: 180e188. doi: 10.1016/j.cej.2019.02.146

Chakraborty S, De S, DasGupta S, Basu JK (2005) Adsorption study for the removal of a basic dye: experimental and modeling. *Chemosphere* 58: 1079–1086. doi: 10.1016/j.chemosphere.2004.09.066

Cheung CW, Porter JF, McKay G (2000) Elovich equation and modified second-order equation for sorption of cadmium ions onto bone char. *Journal of Chemical Technology & Biotechnology* 75: 963-970. doi: 10.1002/1097-4660(200011)75:11%3c963:AID-JCTB302%3e3.0.CO;2-Z

Dubinin MM, Zaverina E, Radushkevich L (1947) Sorption and structure of active carbons. I. Adsorption of organic vapors. Zhurnal Fizicheskoi Khimii *21*: 151-162.

El-Kassimi A, Regti , Laamari, MR, El-Haddad M (2018) Adsorptive removal of anionic dye from aqueous solutions using powdered and calcined vegetables wastes as low-cost adsorbent. *Arab Journal of Basic and Applied Sciences* 25: 93-102. doi: 10.1080/25765299.2018.1517861

Elwakeel KZ, Elgarahy AM, Elshoubaky GA, Mohammad SH (2020a) Microwave assist sorption of crystal violet and Congo red dyes onto amphoteric sorbent based on upcycled sepia shells. *Journal of Environmental Health Science and Engineering* 18: 35–50. doi: 10.1007/s40201-019-00435-1

Elwakeel KZ, Shahat A, Khan ZA, Alshitari W, Guibal E (2020b) Magnetic metal oxide-organic framework material for ultrasonic-assisted sorption of titan yellow and rose bengal from aqueous solutions. *Chemical Engineering Journal* 392: 123635. doi: 10.1016/j.cej.2019.123635

Foroutan R *et al.* (2021) Adsorption of crystal violet dye using activated carbon of lemon wood and activated carbon/Fe3O4 magnetic nanocomposite from aqueous solutions: a kinetic, equilibrium and thermodynamic study. *Molecules* 26: 2241. doi: 10.3390/molecules26082241

Freundlich H (1907) Über die adsorption in lösungen. *Zeitschrift für physikalische Chemie* 57: 385-470.

Gao Q, Xu J, Bu XU (2019) Recent advances about metal–organic frameworks in the removal of pollutants from wastewater. Coord Chem Rev 378: 17-1. doi: 10.1016/j.ccr.2018.03.015

Ghime D, Goru P, Ojha S, Ghosh P (2019) Oxidative decolorization of a malachite green oxalate dye through the photochemical advanced oxidation processes. *Glob Nest J* 21: 195–203. doi: 10.30955/gnj.003000.

Ho YS, McKay G (1999) Pseudo-second order model for sorption processes. *Process Biochemistry* 34: 451-465. doi: 10.1016/S0032-9592(98)00112-5.

Homagai PL, Poudel R, Poudel S, Bhattarai A (2022) Adsorption and removal of crystal violet dye from aqueous solution by modified rice husk. *Heliyon* 8: e09261. doi: 10.1016/j.heliyon.2022.e09261.

Huang, Y., and Zhu, Q. (2015). Computational modeling and theoretical calculations on the interactions between spermidine and functional monomer (methacrylic acid) in a molecularly imprinted polymer. *Journal of Chemistry*, *2015*(1), 216983. doi: 10.1155/2015/216983

Idris-Hermann KT, Raoul TTD, Giscard D, Gabche AS (2018) Preparation and characterization of activated carbons from bitter kola (Garcinia kola) nut shells by chemical activation method using H_3PO_4; KOH and $ZnCl_2$. *Chem Sci Int J* 23: 1–15. doi: 10.9734/CSJI/2018/43411

Kapdan IK, Ozturk R (2005) Effect of operating parameters on color and COD removal performance of SBR: sludge age and initial dyestuff concentration. *J Hazard Mater* B123: 217–222. doi: 10.1016/j.jhazmat.200.5.04.013

Kasera N, Gillikin E, Kolar P *et al.* (2023) Feasibility of nitrate adsorption from aqueous solution by nitrogen and oxygen-modified pine bark biochar: experimental and computational approach. *Discov Water* 3: 13. doi: 10.1007/s43832-023-00037-x

Kaur P, Singh J, Kaur M, Rasane P, Kaur S, Kaur J, Nanda V, Mehta C.M, Sowdhanya D. (2022). Corn Silk as an Agricultural Waste: A Comprehensive Review on Its Nutritional Composition and Bioactive Potential. *Waste and Biomass Valorization* 14, 1-20. doi: 10.1007/s12649-022-02016-0

Khnifira M, El Hamidi S, Sadiq M, Şimşek S, Kaya S, Barka N, Abdennouri M (2022) Adsorption mechanisms investigation of methylene blue on the (0 0 1) zeolite 4A surface in aqueous medium by computational approach and molecular dynamics. *Applied Surface Science* 572: 151381.
doi: 10.1016/j.apsusc.2021.151381

Kolodynska D, Krukoswska-Bak J, Kazmierczak-Razna J *et al*. (2017) Uptake of heavy metal ions from aqueous solutions by sorbents obtained from the spent ion exchange resins. *Micropor Mesopor Mater* 244: 127–136.
doi: 10.1016/j.micromeso.2017.02.040

Kulal P, Badalamoole V (2020) Magnetite nanoparticle embedded Pectin-graft-poly (N-hydroxyethylacrylamide) hydrogel: evaluation as adsorbent for dyes and heavy metal ions from waste water. *Int J Biol Macromol* 156: *1408–1417*.
doi: 10.1016/j. ijbiomac.2019.11.181

Lagergren SK (1898) About the theory of so-called adsorption of soluble substances. Kungliga Svenska Vetenskapsakademiens Handlingar 24: 1-39.

Langmuir I (1918) The adsorption of gases on plane surfaces of glass, mica and platinum. *Journal of the American Chemical society* 40: 1361-1403.
doi: 10.1021/ja02242a004

Lata S (2017) Studies on removal of malachite green dye from aqueous solution using plant-based biosorbents. M.Sc. Thesis, National Institute of Technology, Rourkela.

Monash P, Pugazhenthi G (2009) Adsorption of crystal violet dye from aqueous solution using mesoporous materials synthesized at room temperature. *Adsorption* 15: 390–405.
doi: 10.1007/s10450-009-9156-y

Navarro P, Zapata JP, Gotor G, Gonzalez-Olmos R, Gómez-López VM (2019) Degradation of malachite green by a pulsed light/H2O2 process. *Water Sci Technol* 79: 260–269.
doi: org/10.2166/wst.2019.041

Okoli CP, Guo, QJ, Adewuyi GO (2014) Application of quantum descriptors for predicting adsorption performance of starch and cyclodextrin adsorbents. *Carbohydrate polymers* 101: 40-49.
doi: 10.1016/j.carbpol.2013.08.065

Oninla VO, Awokoya KN, Babalola JO, Balogun KI, Ismail OS (2022) Optimization of synthesis conditions for graft copolymerization of methacrylic acid onto *Garcinia kola* pods and use in the sequestration of cationic dyes from simulated wastewaters. *Biomass Conversion and Biorefinery*
doi: 10.1007/s13399-022-03443-8

Padowski JC, Gorelick SM, Thompson BH, Rozelle S, Fendorf S (2015) Assessment of human–natural system characteristics influencing global freshwater supply vulnerability. Environ Res Lett 10: 104014.
doi: 10.1088/1748-9326/10/10/104014

Platts JA, Baker RJ (2020) A computational investigation of orbital overlap versus energy degeneracy covalency in $[UE_2]^{2+}$ (E= O, S, Se, Te) complexes. Dalton Transactions 49: 1077-1088.
doi: 10.1039/C9DT04484A

Obot I, Macdonald D, Gasem Z (2015) Density functional theory (DFT) as a powerful tool for designing new organic corrosion inhibitors: Part 1: an overview. *Corros Sci* 99: 1–30.
doi: 10.1016/j.corsci.2015.01.037

Ozola-Davidane R, Burlakovs J, Tamm T, Zeltkalne S, Krauklis AE, Klavins M (2021) Bentonite-ionic liquid composites for Congo red removal from aqueous solutions. *J Mol Liq* 337: 116373.
doi: 10.1016/j.molliq.2021.116373

Roland RM, Bhawani SA, Wahi R, Ibrahim MNM (2019) Synthesis, characterization, and application of molecular imprinting polymer for extraction of melamine from spiked milk, water, and blood serum. *Journal of Liquid Chromatography & Related Technologies*
doi: org/10.1080/10826076.2019.167207

Saleh M, Bilici Z, Kaya M, Yalvac M, Arslan H, Yatmaz HC, Dizge N (2021) The use of basalt powder as a natural heterogeneous catalyst in the Fenton and photo-Fenton oxidation of cationic dyes. *Advanced Powder Technology* 32: 1264–1275. doi: 10.1016/j.apt.2021.02.025

Saleh M, Yalvac M, Arslan H, Dizge N (2022) Investigation of basalt properties as heterogeneous catalyst for Fenton oxidation of textile wastewater. *Clean Soil Air Water* 50: 2000432. doi: 10.1002/clen.202000432

Saleh M, Alterkaoui A, Ozdemir NC, Arslan H, Bilici Z, Dizge N (2023) Adsorption of phosphate ions and reactive red 180 from aqueous solution using thermally activated lemon peels waste. *International Journal of Environmental Science and Technology*. doi: 10.1007/s13762-023-05246-4

Santoso E, Ediati R, Kusumawati Y, Bahruji H, Sulistiono DO, Prasetyoko D (2020) Review on recent advances of carbon-based adsorbent for methylene blue removal from waste water. *Mater Today Chem* 16: 100233. doi: 10.1016/j.mtchem.2019.100233

Sarma GK, Gupta SS, Bhattacharyya KG (2016) Adsorption of crystal violet on raw and acid-treated montmorillonite, K10, in aqueous suspension. *J Environ Manag* 171: 1–10. doi: 10.1016/j.jenvman.2016.01.038

Saxena R, Saxena M, Lochab A (2020) Recent progress in nanomaterials for adsorptive removal of organic contaminants from wastewater. *ChemistrySelect* 5: 335-353. doi: 10.1002/slct.201903542

Sharma PS, D'Souza F, Kutner W (2012) Molecular imprinting for selective chemical sensing of hazardous compounds and drugs of abuse. *TrAC Trends Anal Chem* 34: 59–77. doi: 10.1016/j.trac.2011.11.005

Tan K, Hameed B (2017) Insight into the adsorption kinetics models for the removal of contaminants from aqueous solutions. *J Taiwan Inst Chem Eng* 74: 25–48. doi: org/10.1016/j.jtice. 2017.01.024

Tempkin, M., Pyzhev, V. (1940). Kinetics of ammonia synthesis on promoted iron catalyst. *Acta Phys Chim USSR*, 12, 327.

Tkaczyk A, Mitrowska K, Posyniak A (2020) Synthetic organic dyes as contaminants of the aquatic environment and their implications for ecosystems: A review. *Sci Total Environ* 717: 137222. doi: 10.1016/j.scitotenv.2020.137222.

Wahi RK, Yu WW, Liu YP, Meija ML, Falkner JC, Nolte W, Colvin VL (2005) Photodegradation of Congo Red catalyzed by nanosized TiO_2. *J Molecular Catal A Chem* 242: 48–56. doi: 10.1016/j.molcata.2005.07.034

Weber Jr, WJ, Morris JC (1963) Kinetics of adsorption on carbon from solution. *Journal of the Sanitary Engineering Division* 89: 31-59. doi: 10.1061/JSEDAI.00004.

Wei H, Zhao S, Zhang X, Wen B, Su Z (2021) The future of freshwater access: Functional material-based nano-membranes for desalination. *Mater Today Energy* 22: 100856. doi: 10.1016/j.mtener.2021.100856

Zang H, Wang Y, Liu X, Kong J, Nie C (2012) Preparation of molecular imprinted polymers using bi-functional monomer and bicrosslinker for solid phase extraction of rutin. *Talanta* 93: 172–181. doi: 10.1016/j.talanta.2012.02.008

Zhu G, Cheng G, Wang P, Li W, Wang Y, Fan J (2019) Water compatible imprinted polymer prepared in water for selective solid phase extraction and determination of ciprofloxacin in real samples. *Talanta* 200: 307e315. doi: 10.1016/j.talanta.2019.03.070